

Swirling Jet of Gases Mixture into Vacuum

By

Hakuro OGUCHI, Shun-itsu SATO and Osamu INOUE

Summary: In the present paper we are concerned with a swirling jet of gases mixture into a vacuum, and specifically with the effect of the centrifugal force due to swirling motion on the species separation. Both species-density measurement and flow visualization were made by means of the electron-beam fluorescence technique. An appreciable species separation was found to be achieved by the swirling jet of gases mixture into a vacuum. For comparison with the experimental data, a simple two-dimensional analysis is presented for the swirling flow appearing in a cross section normal to the jet axis.

1. INTRODUCTION

So far many investigations have been made on a single jet of binary gases mixture into a vacuum. In the present paper we are concerned with a swirling jet of gases mixture into a vacuum, and specifically with the effect of the centrifugal force on the species separation.

In the experiment the gases mixture of helium and nitrogen is used as a test gas. A swirling jet is produced by issue of the gases mixture through a vortex generator into a vacuum. Both species-density measurement and flow visualization are made by means of the electron-beam fluorescence technique. It will be shown that the species distributions measured indicate an apparent contrast to those of a single jet of gases mixture.

For comparison with the experimental data, a simple two-dimensional analysis is presented for the swirling flow appearing in a cross section normal to the jet axis. Actual phenomenon is much complicated and essentially three-dimensional, so that the analysis based on simple flow model may in general suggest only a qualitative feature of the flow. In spite of the simplifying analysis, however the results are in a reasonable agreement with the data not only qualitatively but also quantitatively.

2. EXPERIMENTAL APPARATUS AND SWIRLING JET GENERATOR

Most of the experimental apparatus is quite the same as that employed previously in the experiment of the free jet from concentric orifices into a vacuum [1], [2].

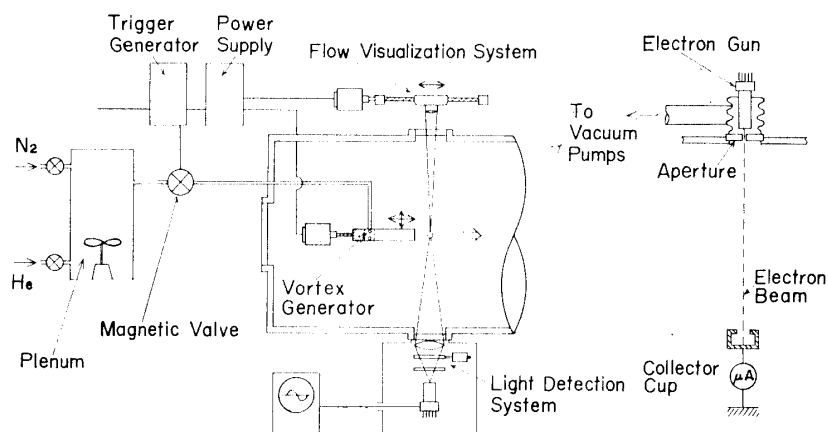


FIG. 1. Schematic diagram of apparatus.

The schematic diagram of the apparatus is shown in Fig. 1. The apparatus consists of (1) a swirling generator, mounted on a drive unit, (2) an electron gun system, (3) an optical system, (4) a flow visualization system with a camera mounted on another drive unit, (5) a gases mixture supply system, and a vacuum system.

In the apparatus a swirling jet generator and gases-mixture supply system are one prepared newly for the present experiment, while the others are the same as employed in the previous experiments. The gases mixture was supplied to the vortex generator from a vessel of capacity 0.5 m^3 , in which a fan is equipped for mixing of two different kinds of gases.

A conventional vortex tube with a slight modification was utilized as a swirling jet generator. The vortex tube is commonly used since Ranque's invention as a device for gas-energy separation; when the gas is supplied to the device, a warmer gas flow is obtained from one opening end of the tube and a colder gas flow from another opening end. For the present purpose a conventional vortex tube was slightly modified so as to suffice for generation of a swirling motion of gases, so that one side of the tube was closed by a flat disk (see Fig. 1).

The electron beam of 16 KV and $300 \mu\text{A}$ was employed for both density measurement and flow visualization. With a fixed beam, the vortex generator was movable by a screw-drive mechanism in the direction either parallel or perpendicular to the jet axis.

3. EXPERIMENTAL CONDITIONS

The gases mixture of nitrogen and helium was used as a test gas. The partial pressures of each components were equal, and fixed at 200 Torr , so that the total pressure of gases mixture was 400 Torr .

The vortex generator was moved normal to the jet axis such that the electron beam could scan over a cross section of the swirling jet. For the case the axial distances x of the cross section from the nozzle exit were chosen to be 10, 20 and

30 mm. For convenience the dimensionless axial distance \bar{x} , referred to the inner diameter d ($=10$ mm) of the nozzle exit is introduced, i.e. $\bar{x} = x/d$.

The capacity of the vacuum system was not sufficient for the continuous issue to maintain the test chamber pressure lower as desired. Therefore the issue of gases mixture was only allowed for a short period, say 0.5 sec. As was checked in the previous experiment the gases issue in such a short period leads so small pressure rise at the test chamber that the experiment may be identified with one under a fixed ambient pressure.

4. SPECIES DENSITY DISTRIBUTIONS OVER VARIOUS CROSS SECTIONS NORMAL TO JET AXIS

The same optical detection system as used in the previous experiment was applied to the species density measurement. The wave length chosen was a line of $5,016 \text{ \AA}$ for helium and a head ($4,278 \text{ \AA}$) of 0-1 band in spectrum of nitrogen. The relation of the luminosity emitted from gases species to its number density was determined by means of a method of the static calibration.

A typical one of oscilloscope records is shown in Fig. 2. The time scale t can easily be deduced to the radial distance r from the jet axis by multiplication of the known driving speed of the generator. The luminosity I can also be deduced to the species number density through the calibration data.

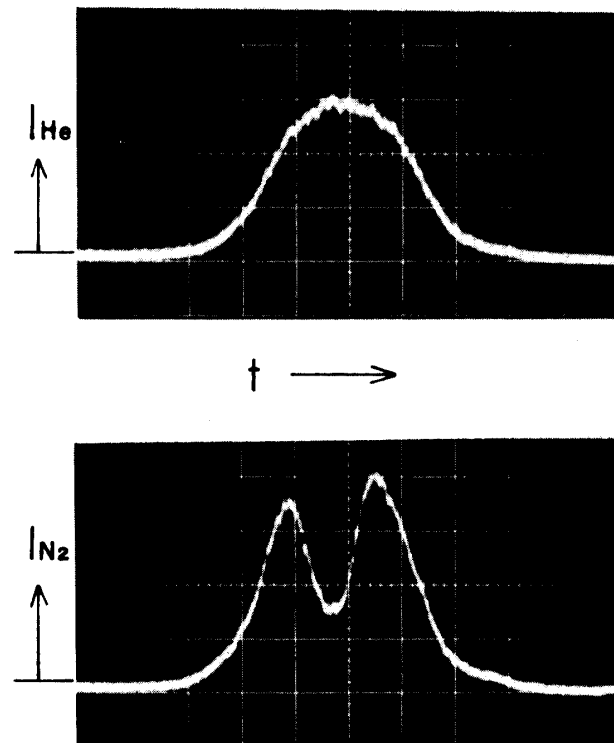


FIG. 2. Luminosity of the gases species in a cross section normal to the jet axis (50 m sec/div.).

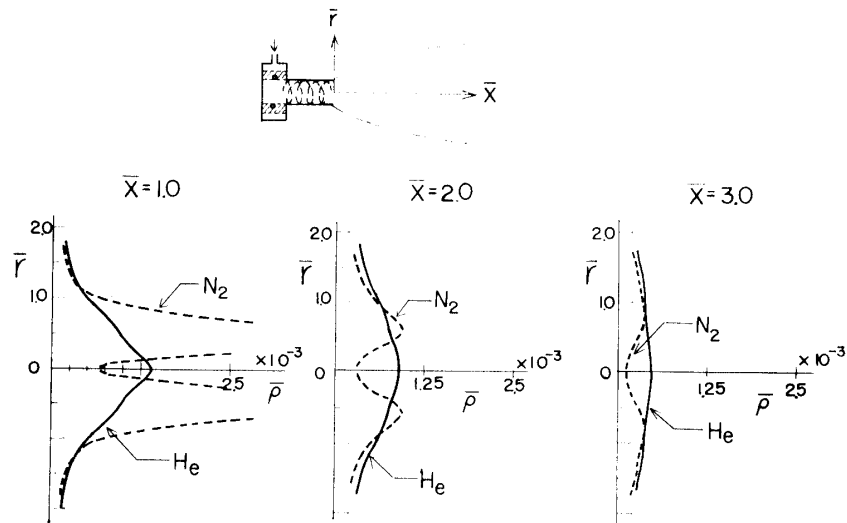


FIG. 3. Density distributions of the gases species in various cross sections normal to the jet axis.

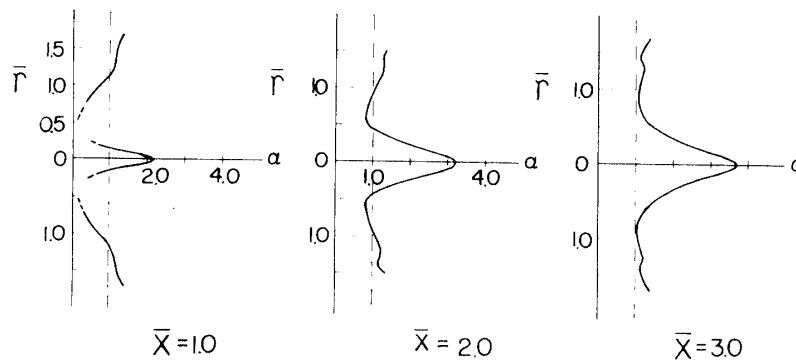


FIG. 4. Distributions of separation factor α .

The species density distributions thus obtained are shown in Fig. 3. As can be seen from the figure, the lighter gas species (helium) is concentrated toward the vicinity of the jet axis, while the heavier gas species (nitrogen) is distributed so as to confine the lighter gas species. This nature is an apparent contrast to that of a jet of gases mixture without swirling; the heavier gas species is enriched near the axis, while the lighter gas species is enriched outside off the axis [3]–[6].

The mass concentration c_i of the i -species is defined by

$$c_i = \rho_i / (\rho_1 + \rho_2)$$

where the subscript “ i ” is 1 for the nitrogen and 2 for the helium, respectively. It should be noted that in the present experiment the gases mixture of nitrogen and helium in equal partial pressures were prepared in the plenum vessel, so that the mass concentration of nitrogen was 0.875.

For convenience we now introduce the separation factor α defined by

$$\alpha = (c_2/c_1) / (c_2/c_1)_s$$

where $()_s$ refers to the value at the plenum vessel, i.e. the stagnation condition. This provides a measure for the degree of species separation. The α -distribution derived from the data, over various cross sections is shown in Fig. 4. It is worthwhile noting that the magnitudes of α on the jet axis are appreciably larger compared to one, and indicate a slight but definite increase toward downstream.

5. TWO-DIMENSIONAL ANALYSIS BASED ON SIMPLE FLOW MODEL AND COMPARISON WITH EXPERIMENT

The expansion flow of gases mixture with swirling motion into a vacuum is so complicated that the straightforward analysis is unlikely to be feasible. In this section, therefore a simple two-dimensional analysis will be proposed to clarify the effect of the centrifugal force on the species separation.

The flow phenomenon of concern is essentially of three-dimensional. There exists no steady two-dimensional swirling flow of the viscous fluid with free boundary, because no driving force can act on the fluid. In view of the above fact, the two-dimensional analysis may provide an approximation to the problem only when the underlying assumptions that will be prescribed in the following are acceptable.

Suppose a cross section of the swirling expansion flow, being normal to the jet axis. The nature of the swirling flow in the cross section may be of a free vortex in a region far from the axis, while it may be of a rigid rotation in a region near the axis. If the transition layer from the rigid rotation to the free vortex is assumed so thin, then the flow field in the cross section is assumed to be divided into two regions; one is the inner flow region near the axis, specified by the rigid rotation, and another is the outer flow region specified by the free vortex (see Fig. 5). If this is the case, the flow field in the cross section may approximately be represented by the solution that can be obtained by simply patching the rigid-rotation solution for the inner region with the free-vortex solution for the outer region.

The boundary between two flow regions, i.e. the edge of rigid rotation, will be determined by imposing an additional condition that the circumferential velocity at the edge is limited to the sound speed of any gases species. In the gases mixture there exist three kinds of sound speed, i.e. two for species and one for mixture. Therefore three kinds of Mach number are defined by referring to each sound speed, i.e.

$$M_i = U/a_i \quad (i=1, 2), \quad M = U/a$$

where a_i and a are the sound speed of the i -species and of the gases mixture. As regards the magnitude of Mach numbers, we have

$$M_1 > M > M_2$$

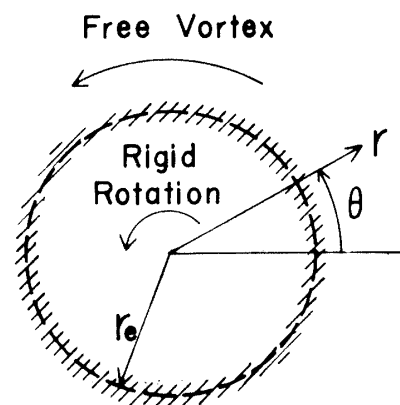


FIG. 5. Schematic diagram of flow model.

if the 1-species is heavier than the 2-species. In the rigid-rotation region the flow Mach number attains its maximum at the edge, and therefore it is reasonable to assume that the Mach number M_1 of the heavier gas at the edge takes the limiting value one, so far as a driving force for swirling is sufficiently great. According to this assumption the condition at the edge is specified by

$$M_1=1 \quad \text{at} \quad r=r_e$$

where r_e is the radial distance of edge from the jet axis.

a) *Solution for rigid-rotation region*

The coordinates (r, θ) are chosen as shown in Fig. 5. The equations of motion governing the two-dimensional swirling motion of gases mixture are

$$\rho \frac{v_\theta^2}{r} = \frac{dp}{dr} \quad (1)$$

$$\frac{d}{dr} \left[\mu \left(\frac{dv_\theta}{dr} - \frac{v_\theta}{r} \right) \right] + \frac{2\mu}{r} \left[\frac{dv_\theta}{dr} - \frac{v_\theta}{r} \right] = 0 \quad (2)$$

where v_θ is the circumferential velocity, p the pressure, ρ the density and μ the viscosity coefficient of the gases mixture.

The continuity equation for the species is

$$\frac{1}{r} \frac{d}{dr} (r \rho_i V_{ri}) = 0 \quad (3)$$

where ρ_i is the i -species density and V_{ri} the radial diffusion velocity of the i -species. The simple integration of Eq. (3) gives

$$V_{ri} = 0 \quad (4)$$

with the condition that V_{ri} must vanish at $r=0$.

In general the diffusion velocity V_{ri} is given by

$$V_{r1} = -D_{12} \left[\frac{1}{c_1} \frac{dc_1}{dr} + \frac{m_2 - m_1}{m} (1 - c_1) \frac{1}{p} \frac{dp}{dr} \right] \quad (5)$$

where D_{12} is the diffusion coefficient, m_i the molecular weight of the i -species, and m the molecular weight of gases mixture [7]. Since $V_{r1} = 0$, we have

$$\frac{1}{c_1} \frac{dc_1}{dr} + \frac{m_2 - m_1}{m} (1 - c_1) \frac{1}{p} \frac{dp}{dr} = 0 \quad (6)$$

The energy equation is

$$\frac{1}{r} \frac{d}{dr} \left(r \kappa \frac{dT}{dr} \right) + C_{P1} D_{12} (\rho_1 V_{r1}) + C_{P2} (\rho_2 V_{r2}) + \mu \left(\frac{dv_\theta}{dr} - \frac{v_\theta}{r} \right) = 0$$

where κ is the heat conductivity, and C_{P_i} is the specific heat of i -species at constant pressure. Since $V_{r_i}=0$, the above equation reduces to

$$\frac{1}{r} \frac{d}{dr} \left(r \kappa \frac{dT}{dr} \right) + \mu \left(\frac{dv_\theta}{dr} - \frac{v_\theta}{r} \right)^2 = 0 \quad (7)$$

The equation of state is

$$p = R \rho T \quad (8)$$

where the gas constant R is related to the species gas constant R_i with the species mass concentration c_i

$$R = c_1 R_1 + c_2 R_2$$

We now introduce the dimensionless variables referred to quantities at the edge of rigid-rotation region;

$$\begin{aligned} v'_\theta &= v_\theta / U, & p' &= p / p_e, & T' &= T_e, \\ \rho' &= \rho / \rho_e, & r' &= r / r_e \end{aligned}$$

where U is the velocity at the edge, and the subscript ‘‘e’’ refers to quantities at the edge. Furthermore, the dimensionless viscosity coefficient and heat conductivity are introduced;

$$\mu' = \mu / \mu_e, \quad \kappa' = \kappa / \kappa_e$$

With the dimensionless quantities introduced above, Eqs. (1), (2), (6) and (7) are rewritten as

$$\frac{dp'}{dr'} = \left(\frac{\rho_e U^2}{p_e} \right) \frac{\rho' v'^2_\theta}{r'} \quad (9)$$

$$\frac{d}{dr'} \left[\mu' \left(\frac{dv'_\theta}{dr'} - \frac{v'_\theta}{r'} \right) \right] + \frac{2\mu'}{r'} \left[\frac{dv'_\theta}{dr'} - \frac{v'_\theta}{r'} \right] = 0 \quad (10)$$

$$\frac{1}{c_1} \frac{dc_1}{dr'} - (1-\lambda)(1-c_1)\gamma_1 M_1^2 \frac{v'^2_\theta}{r' T'} = 0 \quad (11)$$

$$\frac{1}{r'} \frac{d}{dr'} \left(\kappa' r' \frac{dT'}{dr'} \right) + \frac{\mu_1 U^2}{\kappa_1 T_e} \mu' \left(\frac{dv'_\theta}{dr'} - \frac{v'_\theta}{r'} \right)^2 = 0 \quad (12)$$

For abbreviation

$$\lambda = m_2 / m_1, \quad M_1^2 = U^2 / \gamma_1 R_1 T_e \quad (13)$$

where γ_1 is the specific heat ratio of the 1-species.

The boundary conditions are specified as follows:

$$\begin{aligned} v'_\theta = 1, \quad T' = 1, \quad p' = 1 & \quad \text{at } r' = 1 \\ c_1 = c_1(0) & \quad \text{at } r' = 0 \end{aligned}$$

where $c_1(0)$ is a constant.

The solution for Eqs. (9)—(12) can easily be obtained. That is,

$$v'_\theta = r' \quad (14)$$

$$T' = 1 \quad (15)$$

The integration of Eq. (11) after substituting v'_θ and T' obtained above yields

$$c_1 = \frac{a \exp [\gamma_1 M_1^2 (1 - \lambda) r'^2 / 2]}{1 + a \exp [\gamma_1 M_1^2 (1 - \lambda) r'^2 / 2]} \quad (16)$$

where

$$a = c_1(0) / \{1 - c_1(0)\} = c_1(0) / c_2(0)$$

The equation of state becomes

$$p' = (R_1 / R) \rho' R' T' = \lambda / \{1 - (1 - \lambda) c_1\} \rho' R' T'$$

The substitution of ρ' from the above relation into Eq. (9) yields

$$\frac{1}{p'} \frac{dp'}{dr'} = \gamma_1 M_1^2 \frac{\lambda r'}{1 - (1 - \lambda) c_1} \quad (17)$$

With the c_1 given by Eq. (16), the integration of Eq. (17) gives

$$p' = \frac{\exp [\gamma_1 M_1^2 \lambda r'^2 / 2] \{1 + a \lambda \exp [\gamma_1 M_1^2 (1 - \lambda) r'^2 / 2]\}}{\exp [\gamma_1 M_1^2 \lambda / 2] \{1 + a \lambda \exp [\gamma_1 M_1^2 (1 - \lambda) / 2]\}} \quad (18)$$

Consequently all the flow variables in the rigid rotation of gases mixture have been obtained with reference to quantities at the edge of rigid rotation.

b) Free vortex solution for outer region

For the outer flow field far from the axis the viscosity plays no significant role, so that for simplicity the flow there is assumed isentropic. Then we have the free vortex solution for the circumferential velocity v'_θ

$$v'_\theta = 1 / r' \quad (19)$$

The temperature is given by

$$T' = 1 + \frac{1}{2} \frac{U^2}{C_p T_e} (1 - v'^2_\theta)$$

where C_p is the constant-pressure specific heat of gases mixture. In view of the simplicity of the present approximation we shall ignore the dependence of C_p on the

species concentrations. Then the dimensionless temperature becomes

$$T' = 1 + \frac{1}{2}(\gamma_1 - 1)M_1^2(1 - v_\theta'^2) \quad (20)$$

The remaining equations for the outer flow quantities are

$$\frac{1}{c_1} \frac{dc_1}{dr} = (1 - \lambda)\gamma_1 M_1^2(1 - c_1) \frac{v_\theta'^2}{r'T'} \quad (21)$$

$$\frac{1}{p'} \frac{dp'}{dr'} = \frac{\lambda\gamma_1 M_1^2}{1 - (1 - \lambda)c_1} v_\theta'^3 \quad (22)$$

By the use of v_θ' from Eq. (19) and T' from Eq. (20), Eqs. (21) and (22) become, respectively, as follows*:

$$\frac{1}{c_1} \frac{dc_1}{dr'} = (1 - \lambda)\gamma_1 M_1^2(1 - c_1)r'^{-3} \left[1 + \frac{1}{2}(\gamma_1 - 1)M_1^2(1 - r'^{-2}) \right]^{-1} \quad (23)$$

$$\frac{1}{p'} \frac{dp'}{dr'} = \lambda\gamma_1 M_1^2 r'^{-3} [1 - (1 - \lambda)c_1]^{-1} \quad (24)$$

These equations can numerically be solved by the RKG method, starting from the edge $r'=1$ of rigid rotation.

c) Numerical analysis and comparison with experiment

For comparison with the experiment we choose nitrogen as the heavier gas and helium as the lighter gas. The numerical solution has been obtained in the following way. For a given species concentration $c_1(0)$ on the axis $r'=0$, and with $M_1=1$, first the quantities for the inner region were evaluated from the solution of the rigid rotation. With the known c_1 and p' at the edge $r'=1$, the set of the equations (23) and (24) were numerically solved by the RKG method step by step from $r'=1$ toward the outer region. The numerical solutions were obtained for various species-concentrations $c_1(0)$, which were selected to fit the experimental condition.

It should be noted that there exists no geometrical scale to be referred in the two-dimensional flow model, so that the radius r_e of the rigid rotation remains undetermined. Therefore in comparison of the solution with experimental data, the radial scale is adjusted such that both analytical and experimental data fit at

* The solution quite similar to Eqs. (19) and (20) can be obtained for the equations (10) and (12) governing the viscous fluid motion, based on the simplification of $\mu'=\kappa'=1$. That is,

$$v_\theta' = 1/r', \quad T' = 1 + Pr_1(\gamma_1 - 1)M_1^2(1 - v_\theta'^2)$$

where Pr_1 is the Prandtl number of the 1-species. With these expressions for velocity and temperature, the equations for c_1 and p' become quite the same as Eqs. (23) and (24), respectively, in only replacing $(\gamma_1 - 1)/2$ by $Pr_1(\gamma_1 - 1)$. This implies that, for the outer free vortex region, either assumptions of non-viscous isentropic or viscous flow results in a similar type of solution.

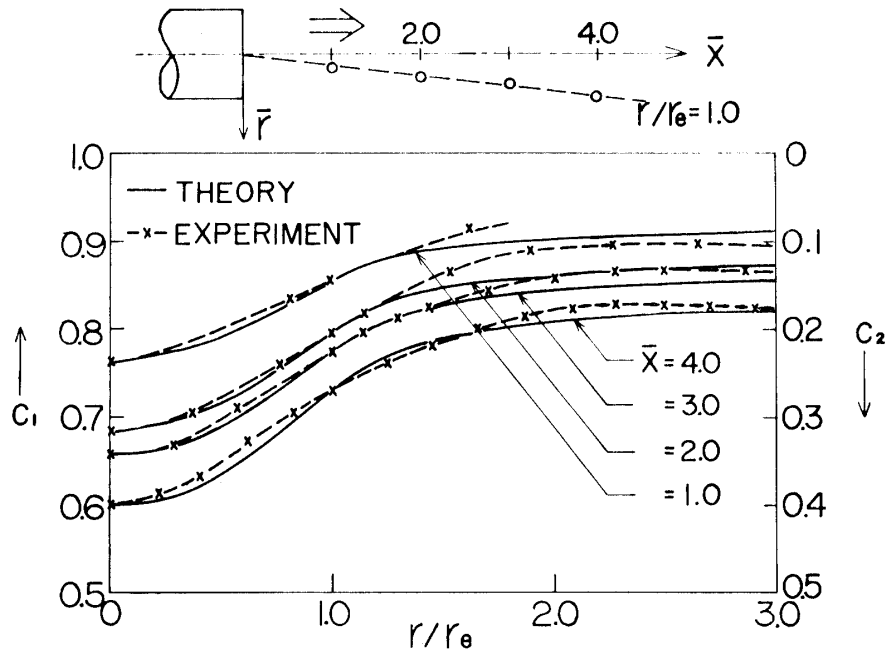


FIG. 6. Distributions of species concentrations c_i and comparison with analytical prediction.

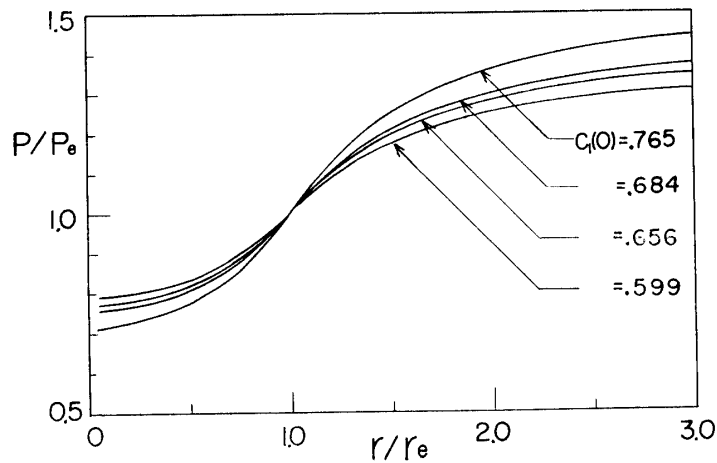


FIG. 7. Pressure distributions predicted by analysis.

the edge $r'=1$ (or $r=r_e$) of the rigid rotation.

The two-dimensional solution thus obtained ensures a continuous matching of the flow variables between inner and outer regions, but fails that of the gradient of flow variables. This defect is inevitable in such a simple two-dimensional analysis as the present one, unless the transitional layer from the rigid rotation to the free vortex is taken into account.

In Fig. 6 shown is the comparison of the numerical solution with the experimental data for the species concentrations. The agreement with the experimental data is reasonable in spite of the simplified flow model of analysis. On the top of Figure 6 shown is the location $r=r_e$ that was determined from comparison of

the experimental data with the numerical solution. This location is identified with the edge of rigid rotation, and there the circumferential velocity attains the sound speed of the heavier species. The feature of the location is remarkable in that the surface $r=r_c$ is nearly conical with an apex near the jet exit.

In the present experiment only the species density was measured, and no other flow variables were measured. In the numerical analysis, all the flow variables can be obtained, and as a reference, the pressure distributions from the analysis are shown in Fig. 7. It is suggested from the figure that the pressure gradient is much greater in the rigid-rotation region than in the outer free-vortex region, so that the rigid rotation plays a significant role for the species separation observed in the present experiment.

6. FLOW VISUALIZATION

The same flow visualization technique as in the previous experiment was employed again. For an electron beam fixed, the nozzle is moved along the jet axis in the direction normal to the beam. In moving with the nozzle, one can view a flow pattern scanned by an electron beam. This was done by moving a camera at a speed fixed relatively to the nozzle and by synchronizing the shutter to open just during the time period between start and stop of the flow. The picture thus taken is shown in Fig. 8. It can be seen from the figure that the edge of the inner core is nearly conical, as was found by the previous analysis (cf. Fig. 6). A feature of flow indicates a distinct contrast to that of an ordinary jet of gases mixture into a vacuum.

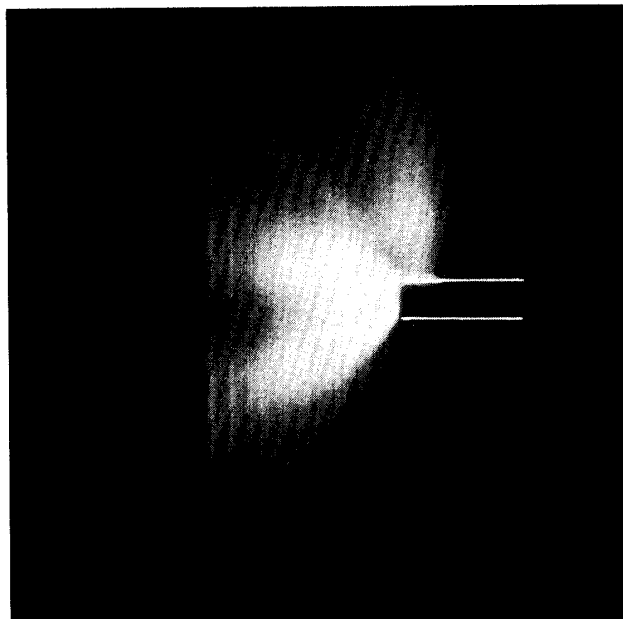


FIG. 8. Flow visualization of gases mixture (helium and nitrogen).

7. CONCLUDING REMARKS

An appreciable species-separation was found to be achieved by a swirling expansion of gases mixture into a vacuum. In the present paper, however the species-separation phenomenon occurring in the vortex generator was not investigated. As regards the separation phenomenon in the vortex tube itself, the gases mixture of air and helium was studied by Suzuki both experimentally and analytically [8]. In his experiment, no appreciable separation was found in the flow within tube. In comparison with the present experiment, the difference is in that the swirling motion of gases is with or without free boundary. The swirling motion of gases appears to be amplified by issue with free boundary into a lower pressure atmosphere. It may be concluded that the swirling motion of gases mixture with free boundary, like a swirling jet expansion into a vacuum, brings on an appreciable degree of species separation. Finally it is expected that the results of the present investigation serve a useful knowledge on development of the devices effective to the species separation of gases mixture.

REFERENCES

- [1] H. Oguchi, S. Sato and O. Inoue, *Trans. Japan Soc. of Aero. Sci.*, **14**, 72 (1971).
- [2] H. Oguchi, S. Sato and O. Inoue, ISAS Report No. 486, Institute of Space and Aero. Sci., University of Tokyo, Vol. 37 (1972).
- [3] E. W. Becker, W. Beyrich, K. Bier, H. Burghoff and F. Zizan, *Z. Naturf.*, **12a**, 609 (1957).
- [4] D. E. Rothe, *Phys. Fluids*, **9**, (1966).
- [5] H. Mikami and Y. Takashima, *Int. J. Heat Mass Transfer*, **11**, 1957 (1968).
- [6] D. I. Sebacher, *AIAA J.*, **6**, 51 (1968).
- [7] S. Chapman and T. G. Cowling, *The Mathematical Theory of Non-Uniform Gases*, Cambridge, the University Press (1939).
- [8] A. Suzuki, *Preprint of Japan Mech. Soc. Engrs.*, No. 700-15 (1970) and No. 710-15 (1971).

*Department of Aerodynamics
Institute of Space and Aeronautical Science
University of Tokyo, Tokyo
September 1, 1972*